J|A|C|S
ARTICLES
Published on Web 07/12/2006

Interaction of α-Synuclein with Divalent Metal Ions Reveals Key Differences: A Link between Structure, Binding Specificity and Fibrillation Enhancement

Andrés Binolfi,[†] Rodolfo M. Rasia,[‡] Carlos W. Bertoncini,[‡,§] Marcelo Ceolin,[||] Markus Zweckstetter,[§] Christian Griesinger,[§] Thomas M. Jovin,[‡] and Claudio O. Fernández*[,†]

Contribution from the Instituto de Biología Molecular y Celular de Rosario, Consejo Nacional de Investigaciones Científicas y Técnicas, Universidad Nacional de Rosario, Suipacha 531, S2002LRK, Rosario, Argentina, Departments of Molecular Biology and NMR-based Structural Biology, Max Planck Institute for Biophysical Chemistry, Am Fassberg 11, D-37077 Göttingen, Germany, and Centro Regional de Estudios Genómicos, Universidad Nacional de La Plata, Calchaquí 23500, Buenos Aires, Argentina

Received March 18, 2006; E-mail: fernandez@ibr.gov.ar

Abstract: The aggregation of α-synuclein (AS) is characteristic of Parkinson's disease and other neurodegenerative synucleinopathies. Interactions with metal ions affect dramatically the kinetics of fibrillation of AS in vitro and are proposed to play a potential role in vivo. We recently showed that Cu(II) binds at the N-terminus of AS with high affinity ($K_d \sim 0.1\ \mu M$) and accelerates its fibrillation. In this work we investigated the binding features of the divalent metal ions Fe(II), Mn(II), Co(II), and Ni(II), and their effects on AS aggregation. By exploiting the different paramagnetic properties of these metal ions, NMR spectroscopy provides detailed information about the protein−metal interactions at the atomic level. The divalent metal ions bind preferentially and with low affinity (millimolar) to the C-terminus of AS, the primary binding site being the ^{119}DPDNEA^{124} motif, in which Asp121 acts as the main anchoring residue. Combined with backbone residual dipolar coupling measurements, these results suggest that metal binding is not driven exclusively by electrostatic interactions but is mostly determined by the residual structure of the C-terminus of AS. A comparative analysis with Cu(II) revealed a hierarchal effect of AS−metal(II) interactions on AS aggregation kinetics, dictated by structural factors corresponding to different protein domains. These findings reveal a strong link between the specificity of AS−metal(II) interactions and the enhancement of aggregation of AS in vitro. The elucidation of the structural basis of AS metal binding specificity is then required to elucidate the mechanism and clarify the role of metal−protein interactions in the etiology of Parkinson's disease.

Introduction

Parkinson's disease (PD) is one of the most common neurodegenerative disorders, affecting about 4 million people worldwide and arising from the progressive loss of dopaminergic neurons in the substantia nigra pars compacta.[1] In the surviving neurons, abnormal proteinaceous aggregates called Lewy bodies and Lewy neurites serve as neuropathological hallmarks of the disease.[2] Point mutations in the α-synuclein (AS) gene cause rare forms of autosomal-dominant familial PD,[3−5] and wild-type AS is the major component of the pathologic lesions characteristic of spontaneous PD.[6] In addition to PD, AS has also been found within intracellular inclusions originated from a diverse group of neurodegenerative disorders,[7] implicating AS in the pathogenesis of an expanding spectrum of diseases referred to as α-synucleinopathies.

α-Synuclein is a 140 amino acid, abundant presynaptic protein, which reversibly associates with membranes via a series of amphipathic α-helices located in its N-terminal region (residues 1−60).[8] A central, hydrophobic domain (NAC, non-Aβ component, residues 61−95) is responsible for the capacity of AS to form β-sheet rich amyloid filaments,[9] followed by an acidic C-terminal tail (residues 96−140) that blocks rapid

[†] Universidad Nacional de Rosario.
[‡] Department of Molecular Biology, Max Planck Institute for Biophysical Chemistry.
[§] Department of NMR-based Structural Biology, Max Planck Institute for Biophysical Chemistry.
[||] Universidad Nacional de La Plata.

(1) Forno, L. S. *J. Neuropathol. Exp. Neurol.* **1996**, *55*, 259−272.
(2) Lewy, F. H., In *Handbuch der Neurologie*; Lewandowsky, M., Abelsdorff, G., Eds.; Springer-Verlag: Berlin, 1912.
(3) Nussbaum, R. L., et al. *Science* **1997**, *276*, 2045−2047.
(4) Kruger, R.; Kuhn, W.; Muller, T.; Woitalla, D.; Graeber, M.; Kosel, S.; Przuntek, H.; Epplen, J. T.; Schols, L.; Riess, O. *Nat. Genet.* **1998**, *18*, 106−108.
(5) de Yebenes, J. G., et al. *Ann. Neurol.* **2004**, *55*, 164−173.
(6) Spillantini, M. G.; Schmidt, M. L.; Lee, V. M.; Trojanowski, J. Q.; Jakes, R.; Goedert, M. *Nature* **1997**, *388*, 839−840.
(7) Goedert, M. *Nat. Rev. Neurosci.* **2001**, *2*, 492−501.
(8) Jao, C. C.; Der-Sarkissian, A.; Chen, J.; Langen, R. *Proc. Natl. Acad. Sci. U.S.A.* **2004**, *101*, 8331−8336.
(9) Giasson, B. I.; Murray, I. V.; Trojanowski, J. Q.; Lee, V. M. *J. Biol. Chem.* **2001**, *276*, 2380−2386.

synuclein filament assembly.[10] We have recently shown that native AS in solution adopts an ensemble of conformations that are stabilized by long-range interactions and act to autoinhibit oligomerization and aggregation.[11−13] Several environmental conditions and ligands have been recognized as triggers for AS fibrillation in vitro, such as high temperature,[14] low pH,[14] polyamines,[15] and metal ions.[16−18] Thus, elucidating the neurochemical factors that lead to AS amyloid deposition is likely to yield valuable insights into the hierarchy of pathophysiological events in PD.

Common features of neurodegenerative disorders include the deposition of misfolded proteins, a process that is dramatically enhanced by metal ions in vitro.[16−19] The data support the hypothesis that metal interactions with the target protein in several of these age-dependent degenerative diseases might constitute one of the major factors contributing to their etiology. Cu(II) and Mn(II) have been implicated in Creutzfeldt-Jakob disease, where the aggregating protein is PrP.[20−23] A role for Cu(II) and Fe(II) is also supported in Alzheimer's disease (AD), in which the aggregating protein is the amyloid β-peptide.[19,20,24−27] Thus, defining binding sites and the molecular details of complex formation may provide important and practical insights into pathogenic processes and neuronal biology. In this connection, the interactions of Cu(II) with the amyloid precursor protein, the amyloid β-peptide, and the prion protein have been very well characterized structurally,[19,26,28−38] and research focused on the interaction of these proteins with Mn(II) constitutes an active area of research.[21,22,39]

Compared with the advances achieved for AD and prion diseases, the role of metal ions in PD (the aggregating protein is AS) is still relatively unexplored. The lack of biochemical, affinity, and structural data at physiologically relevant conditions, as well as the question of which domains of AS are responsible for binding of metal ions, prompted us to investigate the binding of Cu(II) to the full-length AS protein.[16] We found that Cu(II) binds AS with high affinity ($K_d \sim 0.1\ \mu M$) and thereby accelerates AS fibrillation at micromolar concentrations. The high-affinity binding site(s) for Cu(II) is located at the N-terminal domain, specifically the ^{1}MDVFMKGLS^{9} and ^{48}VAHGV^{52} regions. These new findings regarding the structural basis of copper interaction with AS provide a tighter link between PD and other amyloid-related disorders such as AD and prion disease and suggest that perturbations in metal homeostasis may constitute a more widespread element in neurodegenerative disorders than previously recognized.

In addition to the finding of AS as a possible copper-binding protein, other divalent metal ions such as Fe(II) and Mn(II) have been linked to the etiology of PD.[40−42] Cu(II), Fe(II), and Mn(II) quench tyrosine fluorescence and are presumed to form stable metal−protein complexes with AS.[17,40] In vitro studies demonstrated that these cations cause a significant acceleration of AS fibril formation.[17] However, in all cases metal ion concentrations in the millimolar range were used, levels far in excess of those likely to exist in tissues. In light of our findings regarding Cu(II) binding to AS, the relative importance of other divalent metal ions in AS fibrillation needs to be considered. Evaluation of AS−metal(II) interactions at the atomic resolution level is required for this purpose. In this paper we report the structural and binding features of the interaction between AS and the divalent metal ions Fe(II), Mn(II), Co(II), and Ni(II). Adding to the possible biological relevance of Fe(II) and Mn(II), the other divalent metals selected for this study are paramagnetic to different degrees and thus constitute excellent structural probes for achieving a detailed characterization of metal binding sites in AS by nuclear magnetic resonance (NMR) spectroscopy. We have found that the metal ions specified above bind preferentially and with low affinity (millimolar) to the C-terminal region of AS. A comparative analysis with Cu(II) reveals a hierarchy in the binding of metal ions to AS, dictated by structural factors involving different domains of the protein. The influence of divalent metal ions on inducing AS fibrillation was strongly linked to their binding properties. These new

(10) Hoyer, W.; Cherny, D.; Subramaniam, V.; Jovin, T. M. *Biochemistry* **2004**, *43*, 16233−16242.
(11) Bertoncini, C. W.; Jung, Y. S.; Fernandez, C. O.; Hoyer, W.; Griesinger, C.; Jovin, T. M.; Zweckstetter, M. *Proc. Natl. Acad. Sci. U.S.A.* **2005**, *102*, 1430−1435.
(12) Lee, J. C.; Gray, H. B.; Winkler, J. R. *J. Am. Chem. Soc.* **2005**, *127*, 16388−16389.
(13) Lee, J. C.; Langen, R.; Hummel, P. A.; Gray, H. B.; Winkler, J. R. *Proc. Natl. Acad. Sci. U.S.A.* **2004**, *101*, 16466−16471.
(14) Uversky, V. N.; Li, J.; Fink, A. L. *J. Biol. Chem.* **2001**, *276*, 10737−10744
(15) Fernandez, C. O.; Hoyer, W.; Zweckstetter, M.; Jares-Erijman, E. A.; Subramaniam, V.; Griesinger, C.; Jovin, T. M. *EMBO J.* **2004**, *23*, 2039−2046.
(16) Rasia, R. M.; Bertoncini, C. W.; Marsh, D.; Hoyer, W.; Cherny, D.; Zweckstetter, M.; Griesinger, C.; Jovin, T.; Fernández, C. O. *Proc. Natl. Acad. Sci. U.S.A.* **2005**, *102*, 4294−4299.
(17) Uversky, V. N.; Li, J.; Fink, A. L. *J. Biol. Chem.* **2001**, *276*, 44284−44296.
(18) Paik, S. R.; Shin, H. J.; Lee, J. H.; Chang, C. S.; Kim, J. *Biochem. J.* **1999**, *340*, 821−828.
(19) Atwood, C. S.; Moir, R. D.; Huang, X. D.; Scarpa, R. C.; Bacarra, N. M. E.; Romano, D. M.; Hartshorn, M. K.; Tanzi, R. E.; Bush, A. I. *J. Biol. Chem.* **1998**, *273*, 12817−12826.
(20) Brown, D. R.; Kozlowski, H. *Dalton Trans.* **2004**, 1907−1917.
(21) Kim, N. H.; Choi, J. K.; Jeong, B. H.; Kim, J. I.; Kwon, M. S.; Carp, R. I.; Kim, Y. S. *FASEB J.* **2005**, *19*, 783−785.
(22) Gaggelli, E.; Bernardi, F.; Molteni, E.; Pogni, R.; Valensin, D.; Valensin, G.; Remelli, M.; Luczkowski, M.; Kozlowski, H. *J. Am. Chem. Soc.* **2005**, *127*, 996−1006.
(23) Brown, D. R.; Hafiz, F.; Glasssmith, L. L.; Wong, B. S.; Jones, I. M.; Clive, C.; Haswell, S. J. *EMBO J.* **2000**, *19*, 1180−1186.
(24) Miura, T.; Suzuki, K.; Kohata, N.; Takeuchi, H. *Biochemistry* **2000**, *39*, 7024−7031.
(25) Garzon-Rodriguez, W.; Yatsimirsky, A. K.; Glabe, C. G. *Bioorg. Med. Chem. Lett.* **1999**, *9*, 2243−2248.
(26) Bush, A. I., et al. *J. Biol. Chem.* **1999**, *274*, 37111−37116.
(27) Bush, A. I.; Multhaup, G.; Moir, R. D.; Williamson, T. G.; Small, D. H.; Rumble, B.; Pollwein, P.; Beyreuther, K.; Masters, C. L. *J. Biol. Chem.* **1993**, *268*, 16109−10612.
(28) Chattopadhyay, M.; Walter, E. D.; Newell, D. J.; Jackson, P. J.; Aronoff-Spencer, E.; Peisach, J.; Gerfen, G. J.; Bennett, B.; Antholine, W. E.; Millhauser, G. L. *J. Am. Chem. Soc.* **2005**, *127*, 12647−12656.
(29) Garnett, A. P.; Viles, J. H. *J. Biol. Chem.* **2003**, *278*, 6795−6802.
(30) Aronoff-Spencer, E.; Burns, C. S.; Avdievich, N. I.; Gerfen, G. J.; Peisach, J.; Antholine, W. E.; Ball, H. L.; Cohen, F. E.; Prusiner, S. B.; Millhauser, G. L. *Biochemistry* **2000**, *39*, 13760−13771.
(31) Viles, J. H.; Cohen, F. E.; Prusiner, S. B.; Goodin, D. B.; Wright, P. E.; Dyson, H. J. *Proc. Natl. Acad. Sci. U.S.A.* **1999**, *96*, 2042−2047.
(32) Bush, A. I.; Masters, C. L.; Tanzi, R. E. *Proc. Natl. Acad. Sci. U.S.A.* **2003**, *100*, 11193−11194.
(33) Cappai, R., et al. *J. Biol. Chem.* **2003**, *278*, 17401−17407.
(34) Karr, J. W.; Kaupp, L. J.; Szalai, V. *J. Am. Chem. Soc.* **2004**, *126*, 13534−13538.
(35) Karr, J. W.; Akintoye, H.; Kaupp, L. J.; Szalai, V. A. *Biochemistry* **2005**, *44*, 5478−5487.
(36) Belosi, B.; Gaggelli, E.; Guerrini, R.; Kozlowski, H.; Luczkowski, M.; Mancini, F. M.; Remelli, M.; Valensin, D.; Valensin, G. *Chembiochem* **2004**, *5*, 349−359.
(37) Valensin, D.; Mancini, F. M.; Luczkowski, M.; Janicka, A.; Wisniewska, K.; Gaggelli, E.; Valensin, G.; Lankiewicz, L.; Kozlowski, H. *Dalton Trans.* **2004**, 16−22.
(38) Valensin, D.; Luczkowski, M.; Mancini, F. M.; Legowska, A.; Gaggelli, E.; Valensin, G.; Rolka, K.; Kozlowski, H. *Dalton Trans* **2004**, 1284−1293.
(39) Jackson, G. S.; Murray, I.; Hosszu, L. L.; Gibbs, N.; Waltho, J. P.; Clarke, A. R.; Collinge, J. *Proc. Natl. Acad. Sci. U.S.A.* **2001**, *98*, 8531−8535.
(40) Golts, N.; Snyder, H.; Frasier, M.; Theisler, C.; Choi, P.; Wolozin, B. *J. Biol. Chem.* **2002**, *277*, 16116−16123.
(41) Castellani, R. J.; Siedlak, S. L.; Perry, G.; Smith, M. A. *Acta Neuropathol.* **2000**, *100*, 111−114.
(42) Verity, M. A. *Neurotoxicology* **1999**, *20*, 489−497.

insights into the bioinorganic chemistry of PD are crucial to understanding the functional role of protein−metal interactions in the etiology of this disorder and for advancing the design of novel therapeutic strategies.

Experimental Section

Protein and Reagents. Unlabeled and ^{15}N-labeled wild-type AS were prepared as described.[15] $CuSO_4$, $NiSO_4$, $MnCl_2$, $CoCl_2$, and $FeCl_2$ salts of the highest purity available were from Merck or Sigma. The reagents 4-(2-pyridylazo)resorcinol (PAR), Fura-2 pentapotassium salt, and 1,10-phenanthroline were purchased from Sigma, Molecular Probes (Invitrogen), and Fluka, respectively.

Aggregation Assays. AS aggregation measurements were performed with 100 μM AS samples dissolved in buffer A [20 mM sodium 2-(*N*-morpholino)ethanesulfonate (Mes-Na) and 100 mM NaCl, pH 6.5]. Samples were incubated with 100 μM metal at 37 °C under constant stirring. The formation of fibrils was estimated from aliquots (5 μL) taken at different time points by use of the thioflavin-T fluorescence assay.[15,43]

Aggregation yields were normalized to the final values and the averaged data points were fitted to[16]

$$\alpha[t] = (1 - e^{-k_{app}t})/(1 + e^{-k_{app}(t-t_{1/2})}) \quad (1)$$

The quantities k_{app} and $t_{1/2}$ are related to the aggregation reaction as follows:

$$k_{app} = k\epsilon[AS] \quad (2)$$

$$t_{1/2} = \ln(\epsilon[AS]/[nc])/k_{app} \quad (3)$$

where k is the rate constant for incorporation of monomers into growth points located in aggregates, [AS] = total concentration of AS monomer units, [nc] is the concentration of nucleation centers, and ϵ denotes the fraction of addition-competent monomer sites in already formed aggregates. This approximation assumes that [nc] $\ll \epsilon$[AS]. In all cases, the reported $t_{1/2}$ values correspond to the average of at least five independent aggregation measurements.

Binding Assays. Equilibrium dialysis was used to estimate the binding affinities of metals to monomeric AS. One hundred fifty microliters of a 300 μM metal-free AS solution in buffer A was dialyzed for 18 h against the same buffer containing solutions of metals in the 0.1−1.0 mM range. Anaerobic conditions were used in the experiments performed with Fe(II). Co(II) and Ni(II) concentrations were measured by use of 4-(2-pyridylazo)resorcinol (PAR),[44] whereas the fluorescence probe Fura-2 and 1,10-phenanthroline were used for Mn(II) and Fe(II), respectively.[44,45] The calibration curves yielded the relationship [Co(II)] (μM) = (17.3 ± 0.2)ΔA_{514nm}, [Ni(II)] (μM) = (24.4 ± 0.2)ΔA_{514nm}, [Fe(II)] (μM) = (84.0 ± 0.2)ΔA_{500nm}, and [Mn(II)] (μM) = $(1.0 - F/F_0)/0.05$, where F and F_0 are the fluorescence of the Fura-2 probe in the presence and absence of the metal ion, respectively.

Small-Angle X-ray Scattering. SAXS measurements were performed in triplicate on 100 μM AS samples dissolved in buffer A or containing 40−200 μM Cu(II), using the D11A-SAXS (bending magnet) line at the Laboratorio Nacional de Luz Sincrotron, Campinas, Brazil. The wavelength for the incident X-ray beam was 1.488 Å. The sample-to-detector distance was 104 cm. The scattered photons were detected by use of a gas-filled 1D-position sensitive detector. The radius of gyration (R_g) was estimated from the Kratky plots $I(Q)Q^2$ versus Q, where $I(Q)$ is the X-ray scattering intensity and Q is the scattering vector given by $Q = (4\pi \sin\theta)/\lambda$, where 2θ is the scattering angle and λ is the X-ray wavelength.

NMR Spectroscopy. NMR spectra were acquired on a Bruker Avance 600 MHz spectrometer, equipped with cryoprobe. Heteronuclear NMR experiments were performed with pulsed-field gradient (PFG) enhanced pulse sequences on a 100 μM sample of AS in buffer A at 15 °C. Aggregation did not occur under these low-temperature conditions and in the absence of stirring.

For the mapping experiments, ^{1}H−^{15}N HSQC amide cross-peaks affected during metal ion titration were identified by comparing their intensities (I) with those of the same cross-peaks (I_0) in the data set of samples lacking metal ions. The I/I_0 ratios of 95−105 nonoverlapping cross-peaks were plotted as a function of the protein sequence to obtain the intensity profiles. Fe(II) titrations were performed under anaerobic conditions.

Proton longitudinal relaxation rates ($R_1 = 1/T_1$) were measured with the standard inversion recovery pulse sequence, and the paramagnetic relaxation rate enhancement (R_{1p}) was determined on samples containing 5 μM Mn(II) and increasing concentrations of AS (100−800 μM). The Mn(II) binding affinity was estimated according to

$$C_L = C_M(R_{1M}/R_{1p}) - K \quad (4)$$

where C_L is the protein concentration, C_M is the metal ion concentration, R_{1M} is the longitudinal relaxation rate in the paramagnetic site, R_{1p} is the longitudinal relaxation rate enhancement, and K is the dissociation constant.[46] Equation 4 is valid under fast exchange conditions and if the concentration of the AS−Mn(II) complex is always much smaller than C_L. In these cases, from constant C_M, a plot of $1/R_{1p}$ against C_L gives a straight line; R_{1M} is obtained from the slope and K from the intercept on the C_L axis.

PFG-NMR experiments were acquired at 15 °C on unlabeled AS dissolved in D_2O and containing dioxane as an internal radius standard (2.12 Å) and viscosity probe.[47] A series of 20 1D spectra were collected as a function of gradient amplitude. The gradient strength was shifted from 1.69 to 33.72 G cm^{-1} in a linear manner.

Residual dipolar couplings (RDC) were measured on ^{15}N-AS aligned in 5% (w/v) *n*-octylpenta(ethylene glycol)/octanol (C_8E_5).[48] Formation of the anisotropic, dilute liquid crystalline phase was monitored by the splitting of the deuterium signal and ranged on 23 ± 2 Hz. One-bond N−H residual dipolar couplings (D_{NH}) were acquired by use of the 2D inphase−antiphase (IPAP)HSQC sequence under both isotropic and anisotropic conditions.[49]

Acquisition, processing, and visualization of the heteronuclear NMR spectra were performed as previously described.[15,16]

Results

Effect of Divalent Metal Ions on AS Aggregation Correlates with Their Binding Affinity. The time course of AS aggregation in the absence and presence of divalent metal ions was monitored at 37 °C by the standard thioflavin-T fluorescence assay (Figure 1A). We have previously shown that 40−100 μM Cu(II) is effective in accelerating the aggregation of AS (100 μM).[16] To determine whether the other divalent cations could directly affect fibril formation of AS under similar conditions, we monitored the kinetics of aggregation of AS in the presence of 100 μM Mn(II), Fe(II), Co(II), Ni(II), and Cu(II). The characteristic $t_{1/2}$ for aggregation of AS was reduced from ∼65 h to ∼30 h in the presence of 100 μM Cu(II) (Figure 1B).[16] In contrast, no fibrils were observed in the presence of the other divalent metal ions during the first 30 h, indicating

(43) Conway, K. A.; Lee, S. J.; Rochet, J. C.; Ding, T. T.; Williamson, R. E.; Lansbury, P. T., Jr. *Proc. Natl. Acad. Sci. U.S.A.* **2000**, *97*, 571−576.
(44) McCall, K. A.; Fierke, C. A. *Anal. Biochem.* **2000**, *284*, 307−315.
(45) Margerum, D. W.; Banks, C. V. *Anal. Chem.* **1954**, *26*, 200−202.
(46) Bertini, I.; Luchinat, C. *Coord. Chem. Rev.* **1996**, *150*, 1−296.
(47) Wilkins, D. K.; Grimshaw, S. B.; Receveur, V.; Dobson, C. M.; Jones, J. A.; Smith, L. J. *Biochemistry* **1999**, *38*, 16424−16431.
(48) Rückert, M.; Otting, G. *J. Am. Chem. Soc.* **2000**, *122*, 7793−7797.
(49) Delaglio, F.; Grzesiek, S.; Vuister, G. W.; Zhu, G.; Pfeifer, J.; Bax, A. *J. Biomol. NMR* **1995**, *6*, 277−293.

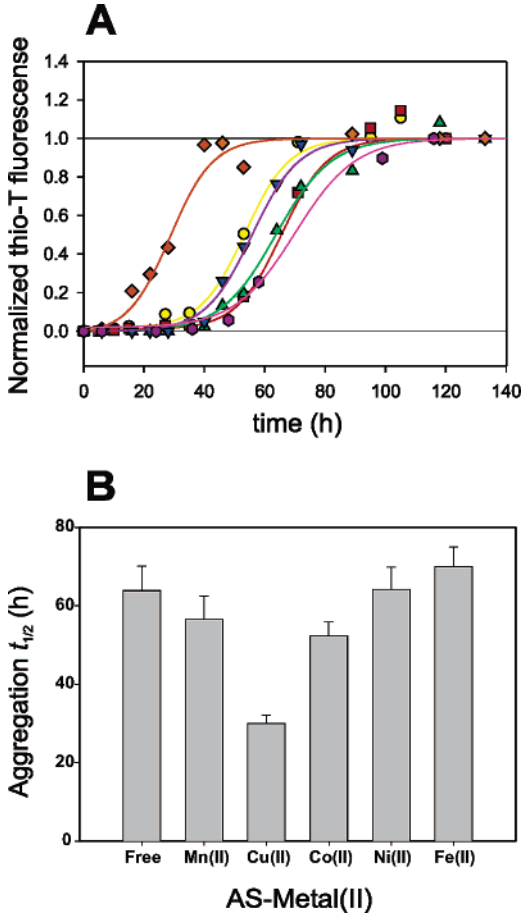

Figure 1. Aggregation kinetics of AS in the presence of divalent metal ions. (A) 100 μM AS in buffer A (green ▲), 100 μM Cu(II) (orange ◆), 100 μM Co(II) (yellow ●), 100 μM Mn(II) (blue ▼), 100 μM Ni(II) (red ■), 100 μM Fe(II) (purple ⬢). Solid lines represent fits to eq 1. (B) Plot of $t_{1/2}$ values (hours) obtained for each metal ion from the fitting procedure in panel A: control (64 ± 7), Cu(II) (30 ± 2), Ni(II) (64 ± 6), Co(II) (53 ± 4), Mn(II) (57 ± 6), and Fe(II) (67 ± 5). Error bars correspond to standard errors of five independent experiments.

that these cations had a minimal or no stimulatory effect on AS fibrillation under these conditions.

To assess whether the absence of fibrillation enhancement by the other divalent metal ions might be linked to a reduced affinity for the protein, we estimated the dissociation constants of the various AS−metal(II) complexes by equilibrium dialysis (Figure S1, Supporting Information). As opposed to the results reported for Cu(II) with this technique (K_d < 1 μM),[16] the dissociation constants estimated for Mn(II), Fe(II), Co(II), and Ni(II) were all in the 1−2 mM range. These results demonstrate that at the low concentrations of metal ions used in the aggregation experiments, the degree of occupancy of the metal binding sites in AS was significant only for Cu(II).

^{1}H NMR of the Interaction between Divalent Metal Ions and AS Reveals Different Spectral Features. Although scarcely populated under the conditions assayed, the AS−metal-(II) complexes could be extensively characterized by NMR due to the paramagnetic nature of the metal ions studied. The range of estimated AS−metal(II) affinities indicates that the metal complexes determined here must have lifetimes substantially shorter than that of Cu(II) at the N-terminus of AS. This also implies that the resonances of the nuclei close to the paramagnetic ions can be more dramatically affected than those in a tight complex [e.g., AS−Cu(II)] due to paramagnetic exchange broadening.[50] The effect serves as a sensitive indicator of the location of the metal ions in the protein structure and has been successfully applied in the characterization of transient metal−protein interactions by NMR.[50]

Changes in the ^{1}H NMR spectra of the side chains of a protein are sensitive probes for detecting metal binding and defining the binding interface.[22,31,36,37,51−53] The ^{1}H NMR spectra of AS in D_2O showed well-resolved clusters of resonances in the 7.0−8.0 ppm range, comprising the side chains of different aromatic residues: His (aa50), Phe (aa4, aa94), and Tyr (aa39, aa125, aa133, aa136) (Figure 2A). The distribution of these residues throughout the AS sequence provides excellent probes for exploring the binding features of metal ions to AS.

Addition of 50 μM Cu(II) to AS caused the selective disappearance of the His50 peak (Figure 2B), whereas further addition of Cu(II) (100 μM) revealed the disruption of the fine scalar-coupling structure of Tyr signals and the disappearance of resonances in the Phe region (Figure 2C). This pattern fully agrees with our previous findings,[16] showing the preferential binding of Cu(II) at the N-terminus (indicated here by the disappearance of His50 and resonances attributed to Phe4) and the low-affinity effects on the C-terminus due to exchange broadening (showed by the broadening of Tyr resonances).

As shown in Figure 2D, the presence of 100 μM Mn(II) caused the selective line broadening of Tyr signals, likely reflecting the preference of this metal ion for the C-terminus. The remaining sharp signals in the cluster centered at 6.6 ppm belong to Tyr 39, as revealed by the 1D spectrum of the C-terminal truncated species (AS 1−108) (data not shown). The spectral features of the 1D ^{1}H NMR of AS in the presence of 100 μM Fe(II) remained almost unperturbed (Figure 2E), as was also the case with 100 μM Co(II) and Ni(II).

Two-Dimensional ^{1}H−^{15}N HSQC Identifies Binding of Divalent Metal Ions to Discrete Regions of AS. To shed light on the structural basis determining the affinity of AS by metal ions, the specific regions of metal binding to AS were mapped by two-dimensional heteronuclear NMR spectroscopy. The ^{1}H−^{15}N heteronuclear single quantum correlation (HSQC) spectra contain one cross-peak for each amide group in the molecule (except those involving prolines) and thus provide sequence-specific probes for locating metal binding sites.[16]

We first recorded a series of ^{1}H−^{15}N HSQC spectra of AS (100 μM) in the presence of increasing levels of Mn(II) (Figures 3 and 4A−C). Substoichiometric concentrations of Mn-(II) were necessary to avoid an excessive broadening of the signals and to minimize chemical exchange effects. Significant changes in cross-peak intensities were observed under these conditions, being restricted to residues located in the C-terminal region of AS. The strongest broadening effects at 10−20 μM Mn(II) corresponded to amide groups of residues Asp 121, Asn122, and Glu123, indicating that this site is the most populated under these conditions (Figure 4A). The paramagnetic

(50) Bertini, I.; Gelis, I.; Katsaros, N.; Luchinat, C.; Provenzani, A. *Biochemistry* **2003**, *42*, 8011−8021.
(51) Syme, C. D.; Nadal, R. C.; Rigby, S. E.; Viles, J. H. *J. Biol. Chem.* **2004**, *279*, 18169−18177.
(52) Stanczak, P.; Valensin, D.; Juszczyk, P.; Grzonka, Z.; Migliorini, C.; Molteni, E.; Valensin, G.; Gaggelli, E.; Kozlowski, H. *Biochemistry* **2005**, *44*, 12940−12954.
(53) Jones, C. E.; Abdelraheim, S. R.; Brown, D. R.; Viles, J. H. *J. Biol. Chem.* **2004**, *279*, 32018−32027.

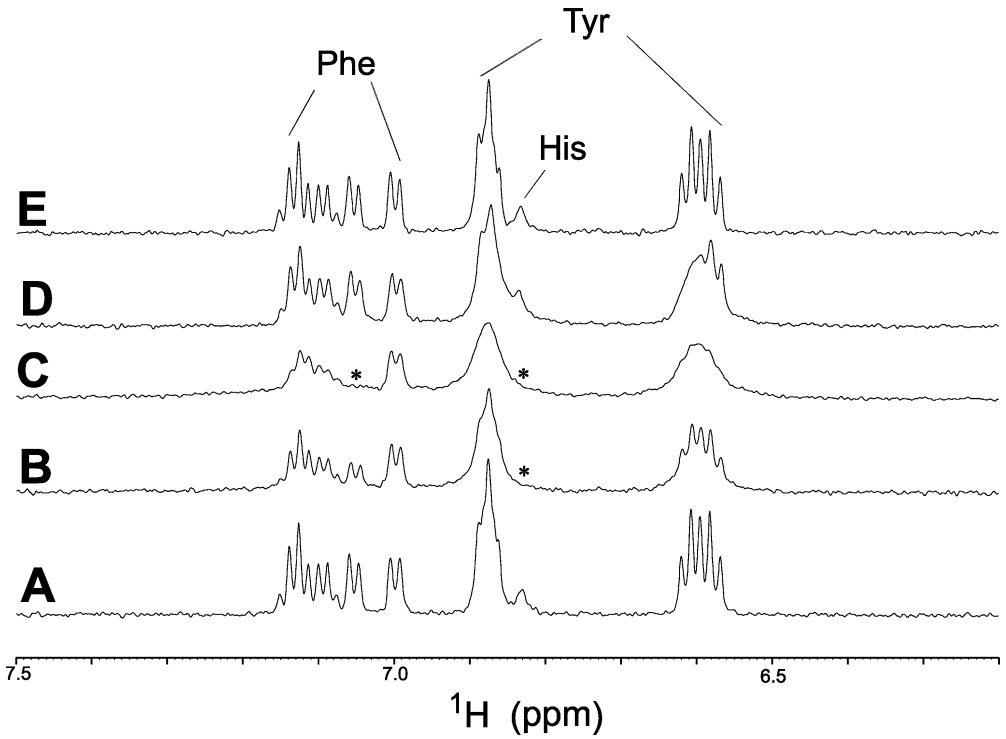

Figure 2. ^{1}H NMR of aromatic side chains of AS in the presence of divalent metal ions. Spectra were registered at 15 °C in D_2O of samples containing 100 μM AS (A), 50 μM Cu(II) (B), 100 μM Cu(II) (C), 100 μM Mn(II) (D), or 100 μM Fe(II) (E). Asterisks indicate peaks broadened beyond detection.

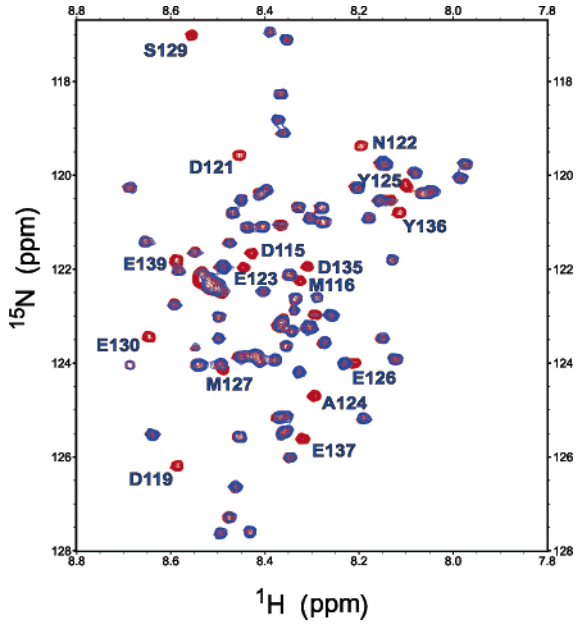

Figure 3. ^{1}H−^{15}N HSQC spectrum of AS in the presence of Mn(II). Overlaid contour plots of the ^{1}H−^{15}N HSQC spectra of 100 μM AS in buffer A, at 15 °C, in the absence (red) and presence (blue) of 100 μM Mn(II). Amino acid residues broadened beyond detection are identified.

effect was further pronounced and generalized at 40−100 μM Mn(II) (Figure 4B,C), likely reflecting an increasing fraction of the metal complex formed around Asp 121, the transient population of secondary sites at the C-terminus, or the occurrence of both processes. Interestingly, the amide resonances assigned to residues located in the N-terminus or belonging to the NAC region remained unaltered even at high Mn(II) concentrations.

An estimation of the binding affinity of Mn(II) to AS was independently obtained by measuring the paramagnetic relaxation enhancement, R_{1p}, induced by low substoichiometric levels of Mn(II) on the Asp121, Asn122, and Glu123 resonances (Figure S2, Supporting Information).[46] Confirming the validity of eq 4 under our experimental conditions, a plot of $1/R_{1p}$ against C_{AS} gives a straight line, from which a dissociation constant of ~1 mM was obtained, consistent with the affinitiy range estimated by equilibrium dialysis.

Titration of AS with Fe(II), Co(II), and Ni(II) showed effects qualitatively similar to those caused by low levels of Mn(II), in that resonances of residues Asp121, Asn122, and Glu123 in the C-terminus were severely affected (Figure 4D−F). However, no generalized line broadening was induced at the C-terminus by 100 μM of added metal ion; overall the spectra remained sharper and the effects were well localized in the 121−123 region. Since the affinities estimated for the AS−metal(II) complexes are similar, the different degree of broadening must be reflecting the magnitude of the electron spin relaxation times (τ_S) of each paramagnetic metal ion [Mn(II) ~ 10^{-8} s, whereas Fe(II), Co(II), and Ni(II) ~ 10^{-11}−10^{-13} s).[46] The cross-peaks of residues located in the NAC region remained insensitive to Fe(II), Co(II), and Ni(II) even at metal:AS ratios of 10:1, whereas a paramagnetic effect centered on His50 was clearly observed for [Fe(II)], [Co(II)] ≥ 500 μM (Figure S3A−C, Supporting Information).

For all the metal ions investigated, the chemical shifts of the amide backbone resonances, when detectable, were essentially unaltered upon metal binding in the range 10−100 μM. Under these conditions, if a 1 mM dissociation constant is assumed, less than 9% of the total protein concentration would be in the metal bound form, obscuring any measurable paramagnetic effect on the chemical shifts. At higher metal-to-protein ratio, as those used for the Co(II), Fe(II), and Ni(II) titrations, chemical shifts perturbations ($\Delta\delta$ ^{15}N ≤ 0.50 ppm) were observed for the most affected resonances at the C-terminus.

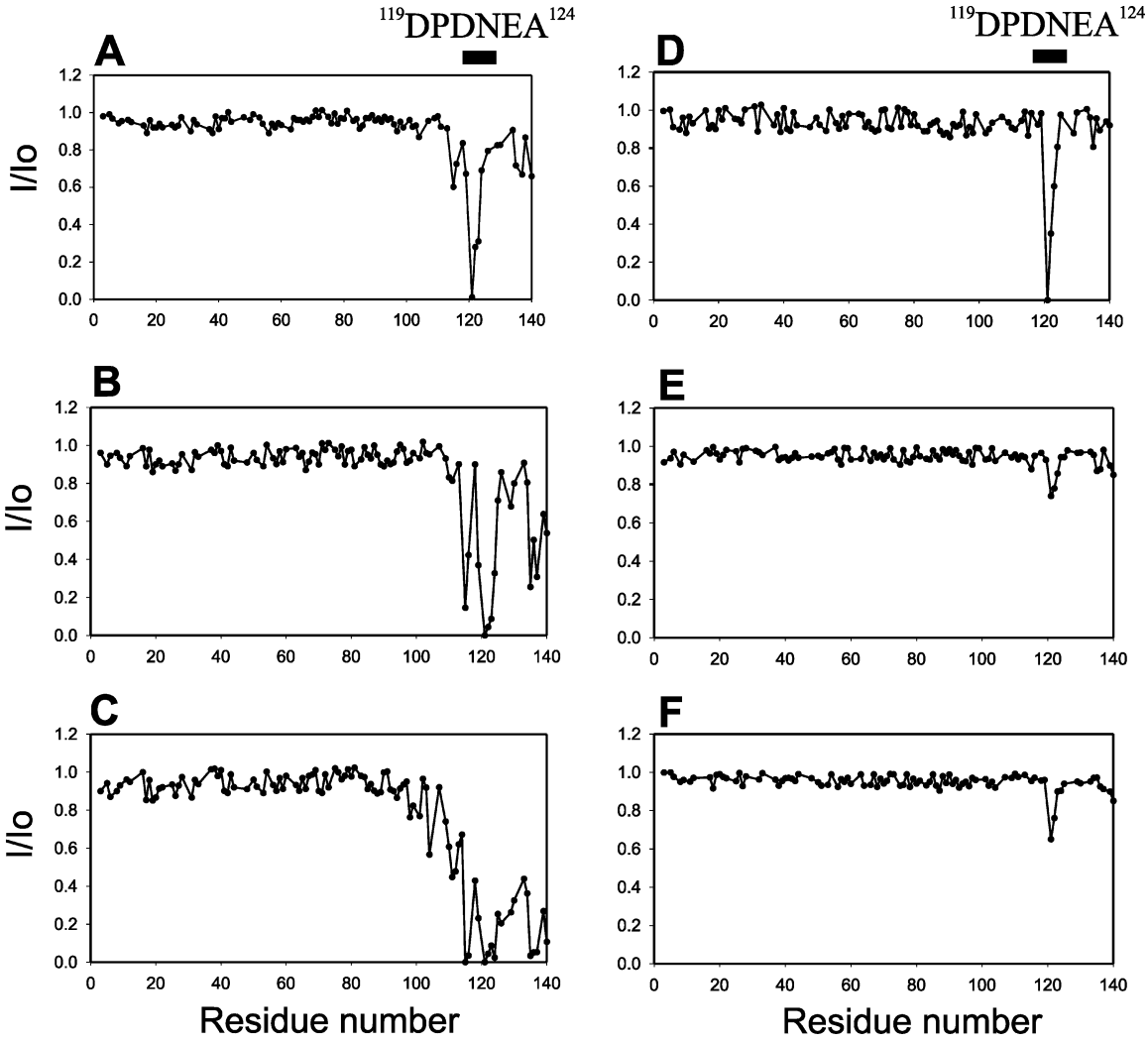

Figure 4. I/I_0 profiles of the backbone amide groups of AS in the presence of divalent metal ions. $^1H-^{15}N$ HSQC spectra of 100 μM AS in buffer A at 15 °C were registered upon addition of (A) 15 μM Mn(II), (B) 40 μM Mn(II), (C) 100 μM Mn(II), (D) 100 μM Co(II), (E) 100 μM Ni(II), or (F) 100 μM Fe(II). N-Terminal region comprises residues 1−60; NAC region, residues 61−95; and C-terminal region, residues 96−140.

Binding of Divalent Metal Ions to the C-Terminus of AS Correlates with the Residual Structure of This Domain. Residual dipolar couplings (RDC) have been successfully used to characterize slow dynamics and domain−domain interactions of the AS monomer.[11,54] As previously reported, the RDC pattern of AS is characterized by the finding of predominantly positive couplings that become exceptionally large for residues 115−119 and 125−129 in the C-terminus (Figure S4, Supporting Information), indicative of the intrinsic residual structure and the higher degree of restricted motions in this domain.[11]

By exploiting the paramagnetic nature and binding features of the studied metal ions, it was possible to conduct experiments (i.e., by use of lower than stoichiometric ratios**)** to pinpoint the primary site of metal ion coordination (Figure 4A−C). Interestingly, upon comparison of the RDC profiles of the AS monomer with the I/I_0 in the presence of low substoichiometric levels of metal ions (Figure 5), a clear correlation was observed between the selective broadening induced by the binding of divalent metal ions to the C-terminus and the intrinsic residual structure identified in that region. The residues constituting the primary metal binding site in the C-terminus, Asp121, Asn122, and Glu123, correspond to the linker sequence showing couplings close to zero and connecting the two major peaks of the RDC profile (115−119 and 125−129). Thus, the binding of divalent metal ions at the C-terminus occurs preferentially in a region that bridges structural elements with restricted motional properties, which are critically stabilized by long-range interactions with other domains.[11]

A Partially Folded Intermediate Is Not Detected for the AS−Cu(II) Interaction. The determination of the hydrodynamic properties of a macromolecule has been extensively applied in the study of conformational changes accompanying molecular association, aggregation, and unfolding.[55−57] As previously reported for AS, conditions that were effective in triggering its aggregation induced changes in the hydrodynamic properties of the protein. At low pH, elevated temperatures, or millimolar concentrations of metal ions, the reduction in the radius of gyration (R_g) of AS was attributed to the formation of a partially folded intermediate.[14,17] We sought evidence for the formation of metal-induced misfolded intermediates of AS by

(54) Bertoncini, C. W.; Fernandez, C. O.; Griesinger, C.; Jovin, T. M.; Zweckstetter, M. *J. Biol. Chem.* **2005**, *280*, 30649−30652.
(55) Jones, J. A.; Wilkins, D. K.; Smith, L. J.; Dobson, C. M. *J. Biomol. NMR* **1997**, *10*, 199−203.
(56) Altieri, A. S.; Hinton, D. P.; Byrd, R. A. *J. Am. Chem. Soc.* **1995**, *117*, 7566−7567.
(57) Pan, H.; Barany, G.; Woodward, G. *Protein Sci.* **1997**, *6*, 1985−1992.

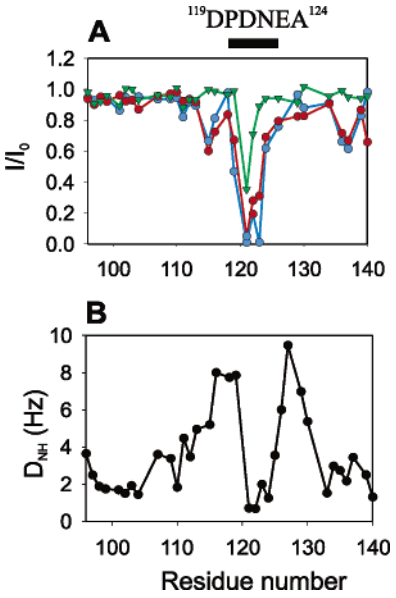

Figure 5. RDC and I/I_0 profiles of backbone amide groups in the C-terminal region of AS (residues 96−140) (A) I/I_0 profiles of the $^1H-^{15}N$ HSQC NMR signals of 100 μM AS in buffer A at 15 °C upon addition of 15 μM Mn(II) (red ●), 15 μM Cu(II) (blue ●), or 40 μM Co(II) (green ▼). The I/I_0 profile reported for Cu(II) and included in this comparison was obtained in conditions favoring its binding to the C-terminal region (pH 5.0). (B) Expansion of the $^1H-^{15}N$ RDCs profile of 100 μM AS aligned in C_8E_5 medium at 15 °C.

determining the hydrodynamic properties of the AS−Cu(II) complexes under the assayed experimental conditions. We employed pulsed-field gradient NMR and SAXS spectroscopy to measure the hydrodynamic properties of AS (100 μM) in the absence and presence of Cu(II) (40−200 μM) (Figure 6). The values determined for the protein in its native state were consistent with previous determinations,[14,58] whereas no changes were detected upon addition of Cu(II) (Table 1), suggesting that the interaction did not affect the size of native AS or cause a significant collapse to a more compact species.

Discussion

Divalent metal ions, especially Cu(II), Fe(II), and Mn(II), are considered as risk factors for PD on the basis of clinical and epidemiological studies.[59] The simplest mechanism proposed involves a direct effect of the metal ions on the aggregation of AS.[17] In this work we sought to delineate the effects of divalent metal ions on the native state of AS by mapping their binding sites and analyzing the consequences of the metal−protein interactions on the aggregation kinetics of AS. A primary difference between Cu(II) and the other divalent ions studied relates to the capability of accelerating the kinetics of AS aggregation.[16,17] As previously reported,[16] Cu(II) was very effective even in the micromolar range of metal concentration, a property that was not shared by the other divalent metal ions. The effectiveness in inducing AS fibrillation correlated with the different ranges of affinities estimated for the binding of metal ions to AS (Table 1). These findings lead to a new conceptual scheme according to which the hierarchy of metal−AS interactions reflects both biological and structural effects, the latter resulting from the nature of the coordinating moieties of the protein, as discussed below.

The NMR analysis of the AS−metal(II) complexes indicated that the divalent metal ions studied bind preferentially to the C-terminal domain of AS in its native state (Figure 4). We conclude that a common, multiple binding site(s) for metal ions exists in the region comprising residues 110−140, which also constitutes the binding interface for polycationic polyamines.[15] Exploiting the different degree of paramagnetism of the metal ions or using substoichiometric metal-to-protein ratios, we identified the primary site for metal ion coordination. The metal interaction was localized on residues Asp121, Asn122, and Glu123, the spectral features of the former being the most affected. This picture is very similar to that determined for the AS−Cu(II) complexes formed at low pH, a condition favoring Cu(II) binding to the C-terminus.[16] Altogether, the data prove conclusively that (i) the divalent metal ions studied here bind preferentially to the C-terminus of AS; (ii) the binding takes place primarily in a well-defined region, likely involving Asp121 as the main anchoring residue; and (iii) AS binds metal ions to the C-terminus with very low selectivity.

A coordination site formed mostly by carboxylate moieties is in agreement with the modest affinity constants observed for metal binding to the C-terminus of AS and thus the high levels of metal ions, except Cu(II), required to induce the aggregation of AS.[17] A similar weak binding was determined for the interaction between AS and natural polyamines that bind exclusively to the C-terminus of AS and trigger its aggregation. However, in contrast to the polyamines, there exists a weaker metal binding site in the N-terminal region of AS for some divalent metal ions (Figure S3, Supporting Information), which might be involved in the aggregation pathway, for example, by forming transient asymmetrically arranged dimers in which the metal ions serve to bridge multiple binding sites. Presumably, these interactions would be significantly stabilized only at high metal:protein ratios, such as those used to induce the aggregation of AS.[17] On the other hand, some studies propose that the mechanism for metal−AS induced aggregation could involve binding exclusively to the negatively charged carboxylates in the C-terminal region, leading to masking of the electrostatic repulsion and the collapse to a partially folded conformation.[17,18] Although the NMR experiments performed at up to 1 mM concentrations of metal ions did not reveal the formation of such an intermediate, our results support a mechanism of metal-induced aggregation in vitro sharing common features for the divalent metal ions Mn(II), Fe(II), Co(II), and Ni(II), yet indicating that this process differs significantly from that induced by Cu(II).

Adding to the hierarchal effect of AS−metal(II) interactions on the fibrillation kinetics of the protein is the specificity of Cu(II) binding over the other divalent metal ions studied here. The affinity and structural data from our previous work indicated that AS binds Cu(II) with high affinity ($K_d \sim 0.1$ μM).[16] The binding affects the ^{1}MDVFMKGLS^9 and ^{48}VAHGV^{52} regions at the N-terminal domain.[16,60,61] On the other hand, the present work provides compelling evidence for a common low-affinity metal binding interface at the C-terminus. These key differences

(58) Morar, A. S.; Olteanu, A.; Young, G. B.; Pielak, G. J. *Protein Sci.* **2001**, *10*, 2195−2199.
(59) Sayre, L. M.; Perry, G.; Smith, M. A. *Curr. Opin. Chem. Biol.* **1999**, *3*, 220−225.
(60) Kowalik-Jankowska, T.; Rajewska, A.; Wisniewska, K.; Grzonka, Z.; Jezierska, J. *J. Inorg. Biochem.* **2005**, *99*, 2282−2291.
(61) Sung, Y. H.; Rospigliosi, C.; Eliezer, D. *Biochim. Biophys. Acta.* **2006**, *1764*, 5−12.

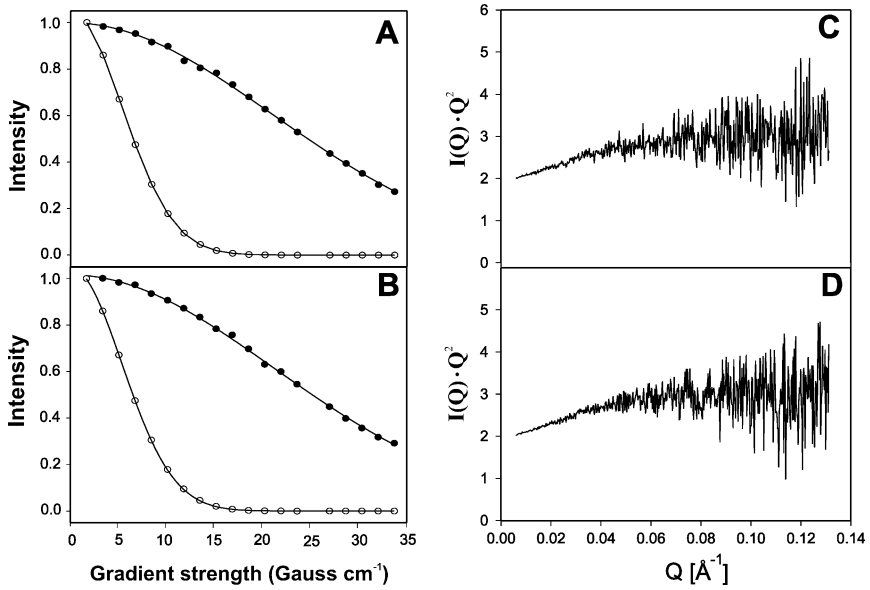

Figure 6. Hydrodynamic properties of AS in the presence of Cu(II) from pulsed-field gradient NMR and SAXS measurements. Plots of the signal intensities (●, aromatic region; ○, dioxane peak) versus the gradient strength for 100 μM AS and 1.2 mM dioxane at 15 °C in D_2O in the absence (A) and presence (B) of 200 μM Cu(II). Also shown are Kratky plot representations of the results of small-angle X-ray scattering analysis of 100 μM AS in buffer A at 15 °C in the absence (C) and presence (D) of 200 μM Cu(II).

Table 1. Aggregation, Affinity, and Structural Features of AS−Metal(II) Interactions

	aggregation and affinity		hydrodynamic properties		primary binding sites	
complex	$t_{1/2}$ (h)	K_d (μM)	R_H (Å)	R_g (Å)	motifs	domain
free	64 ± 7		32.0 ± 0.5	40 ± 2		
Cu(II)	30 ± 2	∼0.1[a]	32.1 ± 0.2	40 ± 2	^{1}MDVFMKGLS^{9}:^{48}VAHGV^{52}	N-terminal
other metals[b]	61 ± 7[c]	∼1000[d]	31.8 ± 0.4[c]	nd[e]	^{119}DPDNEA^{124}	C-terminal

[a] From ref 16. [b] Other metals: Fe(II), Mn(II), Co(II), Ni(II). [c] Reported for other metal ions correspond to the averaged value obtained by considering all metals except Cu(II). [d] Determined by equilibrium dialysis and paramagnetic relaxation enhancement for the AS− metal(II) (Fe, Mn, Co, Ni) and AS−Mn(II) complexes, respectively. [e] Not determined.

in the structural-affinity features of AS−metal(II) interactions reveal a strong link between the specificity of metal binding to AS and the effectiveness in accelerating AS aggregation−fibrillation.

Since elucidation of the residue-specific effects might be central to understand the mechanism of metal-induced fibrillogenesis of AS, we also performed experiments aimed at correlating Cu(II) binding and destabilization of the AS monomer structure. The invariance of the chemical shifts of the backbone amide groups and of the hydrodynamic properties of AS, together with the lack of perturbations in the far UV−CD spectra,[10] indicate the absence of significant conformational changes or the induction of a partially misfolded species. Thus, in the presence of Cu(II), the formation of a complex between Cu(II) and AS, rather than the induction of a partially folded structure, would represent the critical step in the early stage of fibrillation of the protein. As reported for the amyloid β-peptide and prion protein**,** AS is also highly susceptible to metal-catalyzed oxidation, a reaction that induces extensive oligomerization and precipitation of these proteins.[62,63] Since metal-catalyzed oxidation of proteins is a highly selective, site-specific process that occurs primarily at protein sites with transition metal-binding capacity,[64] one can hypothesize that copper binding to the N-terminus of AS renders the protein a relatively easy target (e.g., of oxidative damage) and that the ensuing damage might lead in vivo to a cascade of structural alterations promoting the generation of a pool of AS molecules more prone to aggregate.

It is also instructive to relate the metal binding to AS to other structural features characterizing the AS system. The identification of a similar binding interface for divalent metal ions in the C-terminus of AS suggest a common mode of binding dictated largely by electrostatic interactions. Under these circumstances, the metal ions would more likely interact with carboxylate groups clustered in the protein sequence. This might be the case with the Asp121 binding site, which is surrounded by the aspartic and glutamic acids Asp119, Glu123, and Glu126. A qualitatively similar effect would be expected for the cluster of residues around Asp135, comprising Glu130, Glu131, Glu137, and Glu139. However, a noticeable difference was observed in the metal binding capabilities of the two regions. These discrepancies can be reconciled by comparing the metal binding features with the RDC profile measured for the C-terminal region (Figure 5). By these parameters we found that key tertiary interactions involving the region between residues 105 and 135 restrict the backbone motions on the C-terminus and restrain the conformations populated by this domain.[11] The strong correlation between the location of the primary metal binding site and the dynamic and structural properties inherent to the C-terminal domain suggest that the presence of a specific spatial

(62) Paik, S. R.; Shin, H. J.; Lee, J. H. *Arch. Biochem. Biophys.* **2000**, *378*, 269−277.
(63) Requena, J. R.; Groth, D.; Legname, G.; Stadtman, E. R.; Prusiner, S. B.; Levine, R. L. *Proc. Natl. Acad. Sci. U.S.A.* **2001**, *98*, 7170−7175.
(64) Stadtman, E. R.; Oliver, C. N. *J. Biol. Chem.* **1991**, *266*, 2005−2008.

organization about residues 121−123 might result in a particular orientation of the coordination moieties favoring metal binding to this region. Thus, we propose that binding of metal ions to the C-terminus of AS is not driven exclusively by electrostatic interactions but is mostly determined by the intrinsic conformation of this domain. This view is consistent with recent biochemical and structural studies revealing a role for dynamic and conformational restrictions at the C-terminus in controlling abnormal AS cleavage and degradation in vivo.[54,65] It was recently shown that the generation and accumulation of C-terminal truncated AS might be involved in the initiation and progression of AS aggregation in vivo.[65] In vitro studies have shown endoproteolytic cleavage of AS by proteosomes at Asp119−Pro120 and cleavage of AS by calpain I at Asn122−Glu123.[65−67] In particular, the Asp−Pro peptide bonds are known to be very labile,[68] and thus the presence of a specific spatial organization in this region might act to protect the sole Asp-Pro bond in AS from cleavage. We observed substantial differences in the degree of broadening induced by metal ions on the amide backbone cross-peaks of residues Aps119 and Asp121, located within the ^{119}DPDNEA^{124} fragment, which could reveal a certain degree of hindrance necessary to maintain the ^{119}Asp−Pro^{120} bond in a noncleavable conformation.

Conclusions

By characterizing the NMR features of AS in the presence of divalent metal ions, we have defined metal binding sites and molecular details of complex formation on AS. In particular, we found a hierarchal effect for metal binding to AS, driven by the interaction with specific structural motifs in the N- and C-terminal domains. The effectiveness of divalent metal ions in inducing AS fibrillation is determined by their binding properties. The specificity of Cu(II) binding to AS indicates that the mechanism through which Cu(II) binding impacts on AS aggregation differs significantly from that exerted by other divalent metal ions. We are currently extending these studies to elucidate the structural determinants of metal binding specifity in AS to establish the role of metal ions in synucleinopathies with a molecular resolution comparable to that achieved for other amyloidoses.

Acknowledgment. C.O.F. thanks Fundacion Antorchas, ANPCyT, CONICET, and the Max Planck Society for financial support. C.O.F. is the head of a Partner Group of the Max Planck Institute for Biophysical Chemistry (Göttingen). A.B. is recipient of a fellowship from ANPCyT in Argentina. C.W.B. is supported by a fellowship from the DFG Center for Molecular Physiology of the Brain (CMPB) in Göttingen. C.O.F. and R.M.R. were the recipients of fellowships from the Alexander von Humboldt Foundation. C.O.F. and M.C. are staff members of CONICET. We thank Ms. Kalina Dimova for initial work on the characterization of metal ion binding to α-synuclein. M.C. thanks LNLS, Campinas, Brazil, for SAXS experiments. This work was supported by the CMPB (T.M.J., C.G. and M.Z.), UPMAN (M.Z.), DFG (M.Z.), and the Max Planck Society.

Supporting Information Available: Equilibrium dialysis plots and NMR data including R_1p, I/I_0, and RDC profiles for different As−metal(II) complexes, and complete references 3, 5, 26, 33, and 65. This material is available free of charge via the Internet at http://pubs.acs.org.

JA0618649

(65) Lee, M. K., et al. *Proc. Natl. Acad. Sci. U.S.A.* **2005**, *102*, 2162−2167.
(66) Liu, C. W.; Corboy, M. J.; DeMartino, G. N.; Thomas, P. J. *Science* **2003**, *299*, 408−411.
(67) Mishizen-Eberz, A. J.; Guttmann, R. P.; Giasson, B. I.; Day, G. A., 3rd; Hodara, R.; Ischiropoulos, H.; Lee, V. M.; Trojanowski, J. Q.; Lynch, D. R. *J. Neurochem.* **2003**, *86*, 836−847.
(68) Segalas, I.; Thai, R.; Menez, R.; Vita, C. *FEBS Lett.* **1995**, *371*, 171−175.